

An all-regime and well-balanced Lagrange-projection scheme for the shallow water equations on unstructured meshes

Christophe Chalons, Samuel Kokh and Maxime Stauffert

Abstract We are interested in the numerical approximation of the shallow water equations in two space dimensions. We propose a well-balanced, all-regime and positive scheme. Our approach is based on a Lagrange-projection decomposition which allows to naturally decouple the acoustic and transport terms.

1 Governing equations and asymptotic limit

We consider the numerical approximation of the shallow water equations

$$\begin{cases} \partial_t h + \nabla \cdot (h\mathbf{u}) = 0, \\ \partial_t (h\mathbf{u}) + \nabla \cdot (h\mathbf{u} \otimes \mathbf{u}) + \nabla \frac{gh^2}{2} = -gh\nabla z, \end{cases} \quad (1)$$

where $\mathbf{x} \in \mathbb{R}^2 \mapsto z(\mathbf{x})$ denotes a given smooth topography and $g > 0$ is the gravity constant. Both the water depth h and the velocity $\mathbf{u} = (u_1, u_2) \in \mathbb{R}^2$ depend on the space and time variables, namely $\mathbf{x} \in \mathbb{R}^2$ and $t \in [0, \infty)$. We assume that $h(\mathbf{x}, t = 0) = h_0(\mathbf{x})$ and $\mathbf{u}(\mathbf{x}, t = 0) = \mathbf{u}_0(\mathbf{x})$ are given. We are interested in the design of a numerical scheme that satisfies the well-balanced property, *i.e.* able to strictly preserve the well-known lake at rest solutions such that $h + z = \text{constant}$ and $\mathbf{u} = \mathbf{0}$. For a review on well-balanced numerical schemes, we refer for instance the reader to [2], [8] and the references therein. We also refer to [5] where the authors focus on the 1D case and propose a well-balanced Lagrange-projection strategy. In [3], the proposed Lagrange-projection scheme is fully well-balanced, which means that it preserves a full set of equilibrium solutions (and not only the lake at rest). The

Christophe Chalons, Maxime Stauffert
Laboratoire de Mathématiques de Versailles, UMR 8100, Université de Versailles Saint-Quentin-
en-Yvelines, 78035 Versailles cedex, France, e-mail: christophe.chalons@uvsq.fr

Samuel Kokh
CEA Saclay, 91191 Gif-sur-Yvette, France, e-mail: samuel.kokh@cea.fr

Lagrange-projection methodology is especially well suited for subsonic or near low-Froude number flows. Indeed, it allows to design a natural implicit-explicit strategy which is uniformly stable with respect to the Froude number since the CFL time step restriction is driven by (slow) material waves and not by (fast) acoustic waves, see [6]. Regarding the uniform consistency, we will follow the anti-diffusive technique on the pressure numerical flux introduced in [7] and also used in [4].

The low-Froude limit. Before going further, we give the asymptotic behaviour of the solutions of (1) in the low-Froude limit. With this in mind and as it is customary, we consider the dimensionless quantities $t = t/T$, $\mathbf{x} = \mathbf{x}/L$, $h = h/h_0$, $\mathbf{u} = \mathbf{u}/u_0$ and $z = z/z_0$ where T , L , h_0 , u_0 and z_0 are respectively a reference time, length, water height, velocity and topography of the flow and such that $u_0 = L/T$ and $z_0 = h_0$. Defining the Froude number by $\text{Fr} = u_0/c_0$ where $c_0 = \sqrt{gh_0}$ is the reference sound speed, easy calculations give the dimensionless equations

$$\begin{cases} \partial_t h + \nabla \cdot (h\mathbf{u}) = 0, \\ \partial_t (h\mathbf{u}) + \nabla \cdot (h\mathbf{u} \otimes \mathbf{u}) + \frac{1}{\text{Fr}^2} \nabla p = -\frac{1}{\text{Fr}^2} h \nabla z, \end{cases} \quad (2)$$

where $p(h) = h^2/2$. Assuming that h and z can be written as

$$h = h^{(0)} + h^{(1)}\text{Fr} + h^{(2)}\text{Fr}^2 + \mathcal{O}(\text{Fr}^3) \quad \text{and} \quad \mathbf{u} = \mathbf{u}^{(0)} + \mathbf{u}^{(1)}\text{Fr} + \mathbf{u}^{(2)}\text{Fr}^2 + \mathcal{O}(\text{Fr}^3),$$

we get in particular $p = p^{(0)} + p^{(1)}\text{Fr} + p^{(2)}\text{Fr}^2 + \mathcal{O}(\text{Fr}^3) = p(h^{(0)}) + h^{(1)}h^{(0)}\text{Fr} + \mathcal{O}(\text{Fr}^2)$. Therefore, at order -2 and -1 with respect to the Froude number, (2) gives $\nabla p^{(0)} + h^{(0)}\nabla z = 0$ and $\nabla p^{(1)} + h^{(1)}\nabla z = 0$, which is equivalent to $h^{(0)} + z = H(t)$ and $h^{(1)} = h^{(1)}(t)$, so that the asymptotic behavior is given by

$$\begin{cases} \partial_t h^{(0)} + \nabla \cdot (h^{(0)}\mathbf{u}^{(0)}) = 0, \\ \partial_t (h^{(0)}\mathbf{u}^{(0)}) + \nabla \cdot (h^{(0)}\mathbf{u}^{(0)} \otimes \mathbf{u}^{(0)}) + \nabla p^{(2)} = -h^{(2)}\nabla z. \end{cases} \quad (3)$$

This system is not closed since $p^{(2)}$ and $h^{(2)}$ are not defined. We then consider a bounded domain Ω for the space variable and periodic boundary conditions, so that integrating (3) gives $\partial_t h^{(0)} = 0$ and therefore $h^{(0)} + z = H$ is constant both in space and time. This leads to $\nabla \cdot (h^{(0)}\mathbf{u}^{(0)}) = 0$ and to the low-Froude limit

$$\begin{cases} \nabla \cdot \mathbf{u}^{(0)} = \nabla \cdot \left(\frac{z}{H} \mathbf{u}^{(0)} \right) \\ \left(1 - \frac{z}{H} \right) \partial_t \mathbf{u}^{(0)} + \nabla \cdot (\mathbf{u}^{(0)} \otimes \mathbf{u}^{(0)}) + \frac{1}{H} \nabla p^{(2)} = \nabla \cdot \left(\frac{z}{H} \mathbf{u}^{(0)} \otimes \mathbf{u}^{(0)} \right) - h^{(2)} \nabla \frac{z}{H}. \end{cases} \quad (4)$$

Notice that when the topography is flat, *i.e.* $z = 0$, the classical incompressible Euler equations are recovered.

2 Acoustic-transport decomposition and algorithm

Let us now turn to the acoustic-transport decomposition of (1). If we develop the spatial derivatives and isolate the transport terms $(\mathbf{u} \cdot \nabla)\varphi$, $\varphi = h, h\mathbf{u}$, we can use an

operator splitting with respect to time to obtain the acoustic and transport systems

$$\partial_t h + h \nabla \cdot (\mathbf{u}) = 0, \quad \partial_t (h\mathbf{u}) + h\mathbf{u}(\nabla \cdot \mathbf{u}) + \nabla p = -gh\nabla z, \quad (5)$$

$$\partial_t h + (\mathbf{u} \cdot \nabla)h = 0, \quad \partial_t (h\mathbf{u}) + (\mathbf{u} \cdot \nabla)(h\mathbf{u}) = 0. \quad (6)$$

With these notations, the proposed Lagrange-projection algorithm is defined as follows: for a given discrete state $(h, h\mathbf{u})_j^n$, $j \in \mathbb{Z}$, at time t^n , we define $(h, h\mathbf{u})_j^{n+1}$ at time t^{n+1} by a two-step process namely first update $(h, h\mathbf{u})_j^n$ to $(h, h\mathbf{u})_j^{n+1-}$ by solving (5), and then update $(h, h\mathbf{u})_j^{n+1-}$ to $(h, h\mathbf{u})_j^{n+1}$ by solving (6). By solving we mean here approximating the solution for a period of time Δt . Let us note that if we set $\tau = 1/h$, (5) can be recast into

$$\partial_t \tau - \tau(\mathbf{x}, t) \nabla \cdot \mathbf{u} = 0, \quad \partial_t \mathbf{u} + \tau(\mathbf{x}, t) \nabla p = -\tau(\mathbf{x}, t) \frac{g}{\tau} \nabla z.$$

Following [4], we will choose to discretize (5) thanks to a pressure relaxation

$$\begin{cases} \partial_t \tau - \tau(\mathbf{x}, t) \nabla \cdot \mathbf{u} = 0, \\ \partial_t \mathbf{u} + \tau(\mathbf{x}, t) \nabla \Pi = -\tau(\mathbf{x}, t) \frac{g}{\tau} \nabla z, \\ \partial_t \Pi + \tau(\mathbf{x}, t) a^2 \nabla \cdot \mathbf{u} = \lambda(p^{\text{EOS}}(\tau) - \Pi), \end{cases} \quad (7)$$

with $p^{\text{EOS}}(\tau) = g/(2\tau^2)$, in the limit $\lambda \rightarrow +\infty$. This limit is accounted for by setting $\Pi(\mathbf{x}, t^n) = p^{\text{EOS}}(\tau(\mathbf{x}, t^n))$, and then solving (7) with $\lambda = 0$. We add another approximation by replacing $\tau(\mathbf{x}, t) \partial_{x_r}$ with $\tau(\mathbf{x}, t^n) \partial_{x_r}$, $r = 1, 2$. To sum up, we will define our approximation of (5) by solving (7) over the time interval $[t^n, t^n + \Delta t)$, with $\Pi(\mathbf{x}, t^n) = p^{\text{EOS}}(\tau(\mathbf{x}, t^n))$ and $\lambda = 0$. Note that since (7) and (6) are rotational invariant, it is sufficient to focus on the corresponding quasi-1D systems

$$\begin{cases} \partial_t \tau - \tau(x, t^n) \partial_x u_1 = 0, \\ \partial_t u_1 + \tau(x, t^n) \partial_x \Pi = -\tau(x, t^n) \frac{g}{\tau} \partial_x z, \\ \partial_t u_2 = 0, \\ \partial_t \Pi + \tau(x, t^n) a^2 \partial_x u_1 = 0, \end{cases} \quad (8)$$

and $\partial_t \varphi + u_1 \partial_x \varphi = 0$, $\varphi \in \{h, u_1, u_2\}$, see [4] for more details. Considering a local space step Δx_j , the following discretization strategy of (8) was presented in [5],

$$\begin{cases} \tau_j^{n+1-} = \tau_j^n - \tau_j^n \frac{\Delta t}{\Delta x_j} (u_{j+1/2}^\# - u_{j-1/2}^\#) \\ (u_1)_j^{n+1-} = (u_1)_j^n - \tau_j^n \frac{\Delta t}{\Delta x_j} (\Pi_{j+1/2}^{L,\#} - \Pi_{j-1/2}^{R,\#}) \\ (u_2)_j^{n+1-} = (u_2)_j^n \\ \Pi_j^{n+1-} = \Pi_j^n - \tau_j^n \frac{\Delta t}{\Delta x_j} a^2 (u_{j+1/2}^\# - u_{j-1/2}^\#) \end{cases} \quad (9)$$

where $\Pi_j^n = gh_j^{n2}/2$ and the numerical fluxes $u_{j+1/2}^\#$, $\Pi_{j+1/2}^{L,\#}$ and $\Pi_{j-1/2}^{R,\#}$ are such that $u_{j+1/2}^\# = u_\Delta(\mathbf{U}_j^\#, \mathbf{U}_j^n, \mathbf{U}_{j+1}^\#, \mathbf{U}_{j+1}^n)$, $\Pi_{j+1/2}^{R,\#} = \Pi_\Delta^-(\mathbf{U}_j^\#, \mathbf{U}_j^n, \mathbf{U}_{j+1}^\#, \mathbf{U}_{j+1}^n)$, $\Pi_{j+1/2}^{L,\#} =$

$\Pi_{\Delta}^{\sharp}(\mathbf{U}_j^{\sharp}, \mathbf{U}_j^n, \mathbf{U}_{j+1}^{\sharp}, \mathbf{U}_{j+1}^n)$, where $\mathbf{U} = (h, hu, \Pi, z)^t$ and

$$\begin{aligned}\Pi_{\Delta}(\mathbf{U}_L^{\sharp}, \mathbf{U}_R^{\sharp}) &= \frac{\Pi_L^{\sharp} + \Pi_R^{\sharp}}{2} - a \frac{(u_1)_R^{\sharp} - (u_1)_L^{\sharp}}{2}, \\ u_{\Delta}(\mathbf{U}_L^{\sharp}, \mathbf{U}_L^n, \mathbf{U}_R^{\sharp}, \mathbf{U}_R^n) &= \frac{(u_1)_L^{\sharp} + (u_1)_R^{\sharp}}{2} - \frac{\Pi_R^{\sharp} - \Pi_L^{\sharp}}{2a} - \frac{1}{2a} \{gh\Delta z\}_{\Delta}(\mathbf{U}_L^n, \mathbf{U}_R^n), \\ \Pi_{\Delta}^{\pm}(\mathbf{U}_L^{\sharp}, \mathbf{U}_L^n, \mathbf{U}_R^{\sharp}, \mathbf{U}_R^n) &= \Pi_{\Delta}(\mathbf{U}_L^{\sharp}, \mathbf{U}_R^{\sharp}) \pm \frac{1}{2} \{gh\Delta z\}_{\Delta}(\mathbf{U}_L^n, \mathbf{U}_R^n)\end{aligned}$$

and $\{gh\Delta z\}_{\Delta}(\mathbf{U}_L^n, \mathbf{U}_R^n) = g(h_L^n + h_R^n)(z_R - z_L)/2$. If one chooses $\sharp = n$ (resp. $\sharp = n+1^-$) we get an explicit (resp. implicit) scheme. Note that $\{gh\Delta z\}_{\Delta}$ that accounts for the gravity source term is always evaluated at time t^n . As far as the transport step is concerned, we consider a classic explicit scheme for $\varphi \in \{h, hu_1, hu_2\}$,

$$\varphi_j^{n+1} = \varphi_j^n - \frac{\Delta t}{\Delta x_j} \left(u_{j+1/2}^{\sharp} \varphi_{j+1/2}^{n+1-} - u_{j-1/2}^{\sharp} \varphi_{j-1/2}^{n+1-} \right) - \frac{\Delta t}{\Delta x_j} \varphi_j^{n+1-} \left(u_{j+1/2}^{\sharp} - u_{j-1/2}^{\sharp} \right), \quad (10)$$

with $\varphi_{j+1/2}^{n+1-} = \varphi_j^{n+1-}$ (resp. φ_{j+1}^{n+1-}) if $u_{j+1/2}^{\sharp} \geq 0$ (resp. < 0). In the above formulas, a is taken as a local approximation of the Lagrangian sound speed at each interface, $a_{j+1/2} = 1.01 \max(h_j \sqrt{gh_j}, h_{j+1} \sqrt{gh_{j+1}})$. For the detailed properties of (9)-(10) we refer the reader to [5]. Let us just recall that it is conservative in the usual sense of finite volumes methods. Moreover, the scheme is well-balanced for lake at rest solutions, which means that if $\mathbf{u}_j^n = 0$ and $h_j^n + z_j^n = h_{j+1}^n + z_{j+1}^n$ for all $j \in \mathbb{Z}$, then $h_j^{n+1} = h_j^n$ and $\mathbf{u}_j^{n+1} = \mathbf{u}_j^n$, $j \in \mathbb{Z}$. At last, the time-implicit scheme is stable under a condition which does not depend either on the acoustic system or the sound speed c , but which only depends on the transport step and its material velocity \mathbf{u} . This is of particular interest in the low-Froude regime, since the definition of Δt is uniform with respect to the Froude number.

Truncation error in the low-Froude regime. In this paragraph, we consider the dimensionless shallow-water equations and we motivate a correction to get the uniform consistency. The correction is similar to the one in [7] for low-Mach regimes and we focus on the explicit case $\sharp = n$. In the following we will say that the flow is in the low Froude regime if $\text{Fr} \ll 1$ and $\partial_x p + h \partial_x z = \mathcal{O}(\text{Fr}^2)$. Using the dimensionless quantities, the pressure numerical fluxes write

$$\begin{aligned}\Pi_{j+1/2}^{L,n} &= \frac{\Pi_j^n}{\text{Fr}^2} + \frac{1}{2\text{Fr}^2} \left(\Pi_{j+1}^n - \Pi_j^n + \frac{h_j^n + h_{j+1}^n}{2} (z_{j+1} - z_j) \right) - \frac{a}{2\text{Fr}} (u_{j+1}^n - u_j^n), \\ \Pi_{j+1/2}^{R,n} &= \frac{\Pi_{j+1}^n}{\text{Fr}^2} - \frac{1}{2\text{Fr}^2} \left(\Pi_{j+1}^n - \Pi_j^n + \frac{h_j^n + h_{j+1}^n}{2} (z_{j+1} - z_j) \right) - \frac{a}{2\text{Fr}} (u_{j+1}^n - u_j^n).\end{aligned}$$

If we compute the truncation errors and use the fact that $\Pi_{j+1}^n - \Pi_j^n + (h_j^n + h_{j+1}^n)(z_{j+1} - z_j)/2 = \mathcal{O}(\text{Fr}^2 \Delta x)$, we obtain

$$\begin{aligned}\Pi_{j+1/2}^{L,n} &= \frac{\Pi_j^n}{\text{Fr}^2} + \frac{1}{2\text{Fr}^2} \left(\Pi_{j+1}^n - \Pi_j^n + \frac{h_j^n + h_{j+1}^n}{2} (z_{j+1} - z_j) \right) + \mathcal{O}\left(\frac{\Delta x}{\text{Fr}}\right), \\ \Pi_{j+1/2}^{R,n} &= \frac{\Pi_{j+1}^n}{\text{Fr}^2} - \frac{1}{2\text{Fr}^2} \left(\Pi_{j+1}^n - \Pi_j^n + \frac{h_j^n + h_{j+1}^n}{2} (z_{j+1} - z_j) \right) + \mathcal{O}\left(\frac{\Delta x}{\text{Fr}}\right).\end{aligned}$$

It is thus clear that the consistency errors are not uniform with respect to the Froude number. In order to avoid large errors in the numerical diffusion terms when $\text{Fr} \rightarrow 0$, we suggest to replace the definition of $\Pi_\Delta(\mathbf{U}_L^\#, \mathbf{U}_R^\#)$ by

$$\Pi_\Delta^\theta(\mathbf{U}_L^\#, \mathbf{U}_R^\#) = \frac{\Pi_L^\# + \Pi_R^\#}{2} - \theta(\mathbf{U}_L^\#, \mathbf{U}_R^\#) a \frac{(u_1)_R^\# - (u_1)_L^\#}{2},$$

which, as long as we take $\theta_{j+1/2} = \mathcal{O}(\text{Fr})$, now gives the uniform consistency. In practice, we will set $\theta_{j+1/2} = \min\left(|u_{j+1/2}^n|/\max(c_j, c_{j+1}), 1\right)$.

At last, recall that the scheme easily extends to $2D$ unstructured meshes by rotational invariance. Moreover, it is easily proved that both fully explicit (EXEX) and implicit-explicit (IMEX) schemes are well-balanced also in $2D$.

3 Numerical experiments

We first consider a traveling vortex as in [1]. For this test case we consider a flat bottom and we use a regular cartesian mesh of 160×160 cells that discretizes the physical domain $[0, 1] \times [0, 1]$. The boundary conditions imposed are periodic along the x -direction and absorbing boundaries along the y -direction. The mapping of the velocity magnitude is displayed in Figure 1 and we can observe that the accuracy of the solution is really improved by the low-Froude correction. Furthermore, the accuracy of the solution between the EXEX and the IMEX scheme with low-Froude correction is comparable whereas it took about 100 times less time steps and 10 times less CPU time computation with the IMEX than with the EXEX scheme.

We now consider a non-flat bottom. We extend the physical domain of the traveling vortex test above to the rectangle $[0, 2] \times [0, 1]$. The boundary conditions and initial conditions for h and u are the same as before. However we consider here a topography defined by $z(x, y) = 10 \exp(-5(x-1)^2 - 50(y-0.5)^2)$ following [1].

We compare in Figure 2 the results between EXEX and IMEX schemes, with or without low Froude correction. Here again, the vortex structure of the flow is completely destroyed by numerical diffusion without low-Froude corrections $\theta = \mathcal{O}(\text{Fr})$, with both schemes. Finally, we can remark that the EXEX scheme took about 20 times more iterations and 15 times more CPU times than the IMEX scheme, both with low-Froude correction.

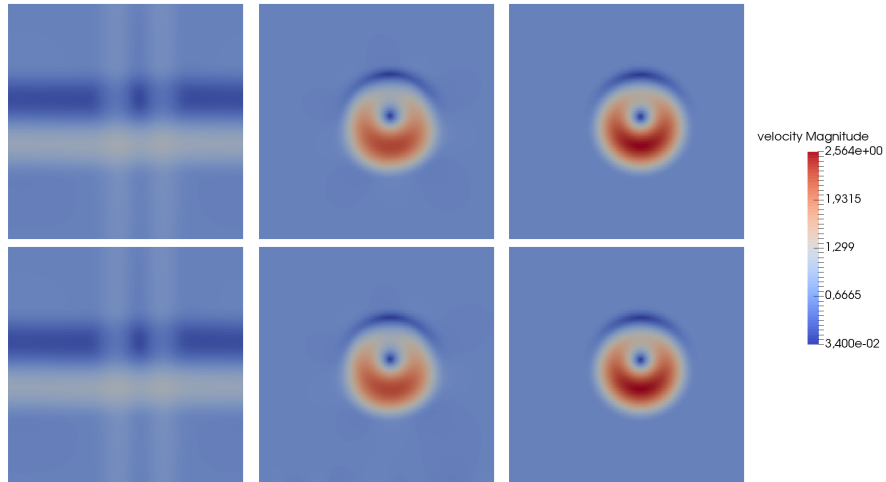


Fig. 1 Flat bottom. Velocity magnitude at final time $T_f = 0.1$ with the EXEX scheme (top) and the IMEX scheme (bottom). $\theta = 1$ (left), $\theta = O(\text{Fr})$ (center) and exact solution (right).

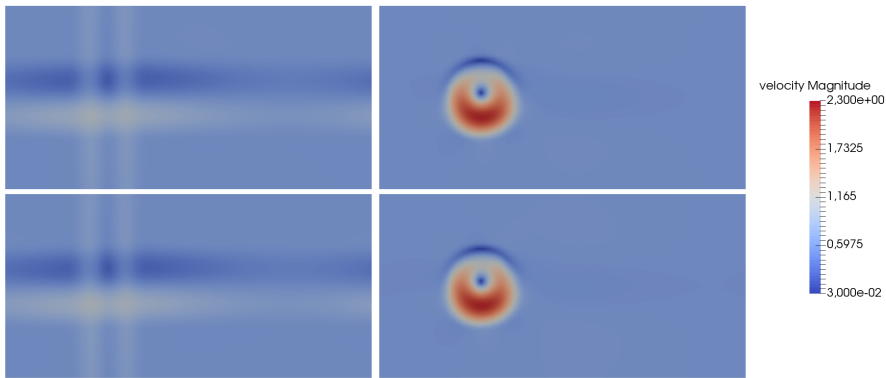


Fig. 2 Non-flat bottom. Velocity magnitude at final time $T_f = 0.1$ with the EXEX scheme (top) and IMEX scheme (bot) with $\theta = 1$ (left) and $\theta = O(\text{Fr})$ (right).

References

1. G. Bispen, K.R Arun, M. Lukacova, S. Noelle, Commun. Comput. Phys., 2014
2. F. Bouchut, Springer Science & Business Media, 2004
3. M.J Castro Díaz, C. Chalons, T. Morales de Luna, SINUM, 2018
4. C. Chalons, M. Girardin, S. Kokh, Commun. Comput. Phys., 2016
5. C. Chalons, P. Kestener, S. Kokh, M. Stauffert, Commun. Math. Sci., 2017
6. F. Coquel, Q. Nguyen, M. Postel, Q. Tran, Math. Comput., 2010
7. S. Dellacherie, J. Comput. Phys., 2010
8. L. Gosse, Springer, 2013